CSIRO

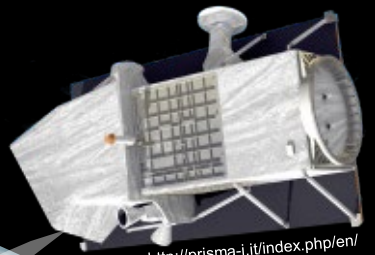

Source: http://prisma-i.it/index.php/en/

Regional-scale mapping of phyllosilicates using the new generation of VNIR-SWIR hyperspectral satellite sensors

Carsten Laukamp, Ian Lau, Heta Lampinen, Morgan Williams, Fang Huang

CSIRO Mineral Resources, Australia

www.csiro.au

Kaolinite - KGa-1b

$Al_2Si_2O_5(OH)_4$

- $\nu+\delta AlOH_{o1}$ intensity increases with kaolinite crystallinity!

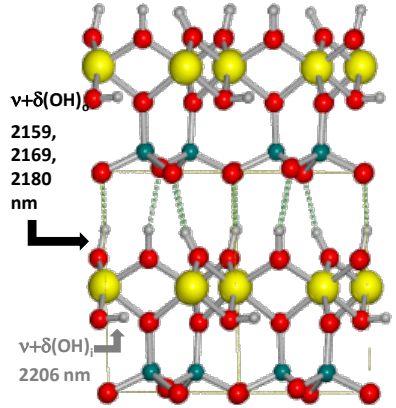

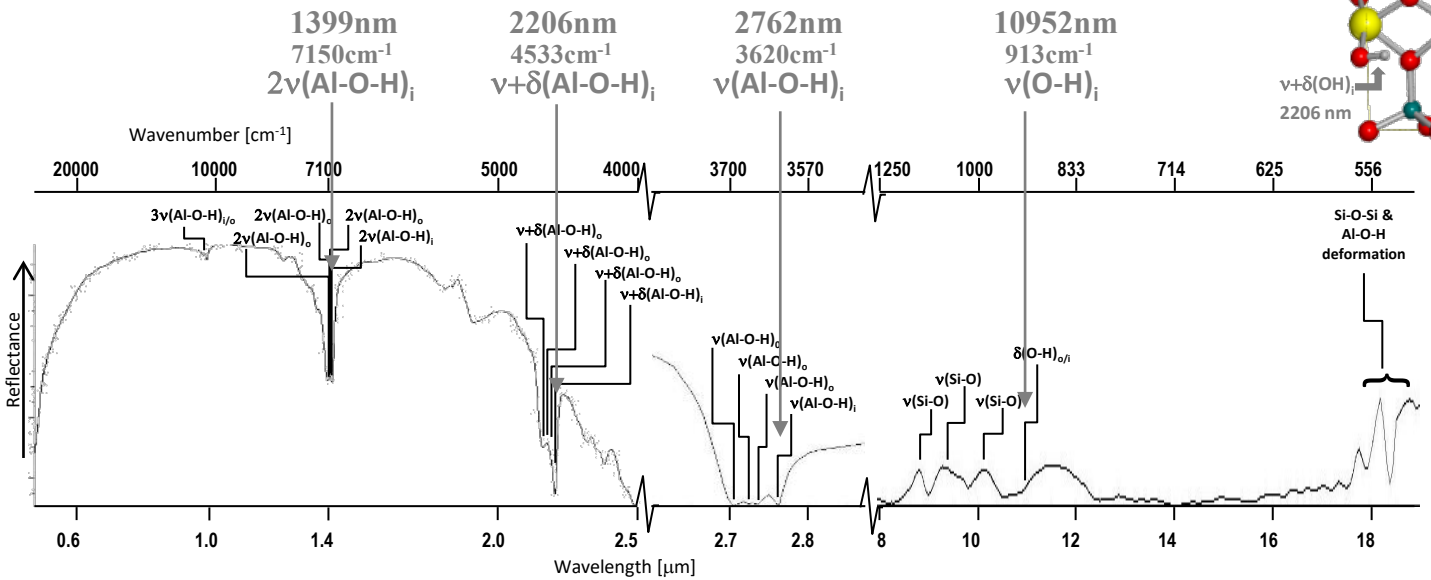

Kaolinite - KGa-1b

$Al_2Si_2O_5(OH)_4$

- $\nu+\delta AlOH_{o1}$ intensity increases with kaolinite crystallinity!

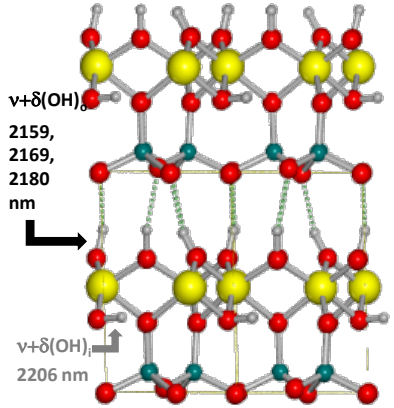

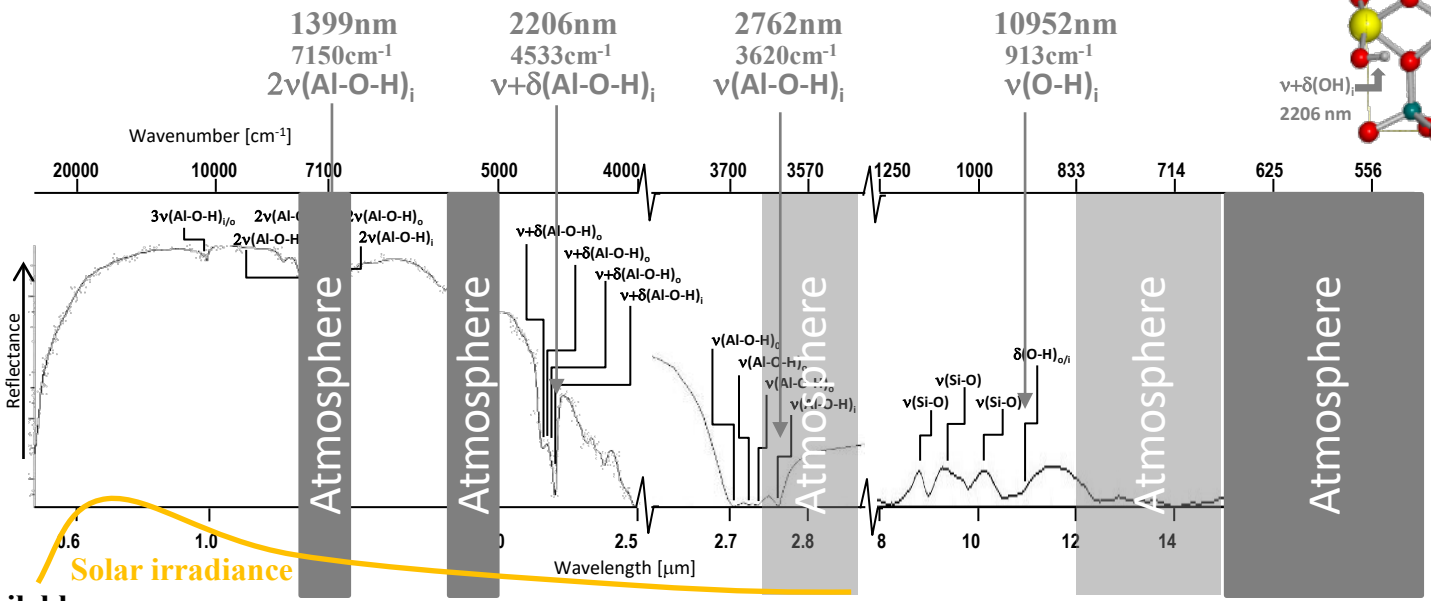

Publicly available hyperspectral satellite imagery

existing — possible? — yes please!

A new fleet of VNIR-SWIR hyperspectral satellites

	PRISMA (ASI)	EnMAP (DLR)	EMIT (NASA/JPL)
Launch date	2019	2022	2022
Range (VNIR/SWIR)	400 – 2500 nm	418.2–2445.5 nm	381-2493 nm
Bands (VNIR/SWIR)	66/173	89/155	285
Sampling dist. (VNIR/SWIR)	9-13/9-14.5 nm	6.4/10.0 nm	~7.5 nm
SNR (VNIR/SWIR)	450to161:1/800to200:1	620:1/230:1	500to1250:1/250to750:1
Pixel size	31 m	30 m	60 m
Swath width	31 km	30 km	75 km
	https://www.asi.it/en/earth-science/prisma/	https://planning.enmap.org/	https://earth.jpl.nasa.gov/emit/data/data-portal/coverage-and-forecasts/

Hyper and multispectral sensors

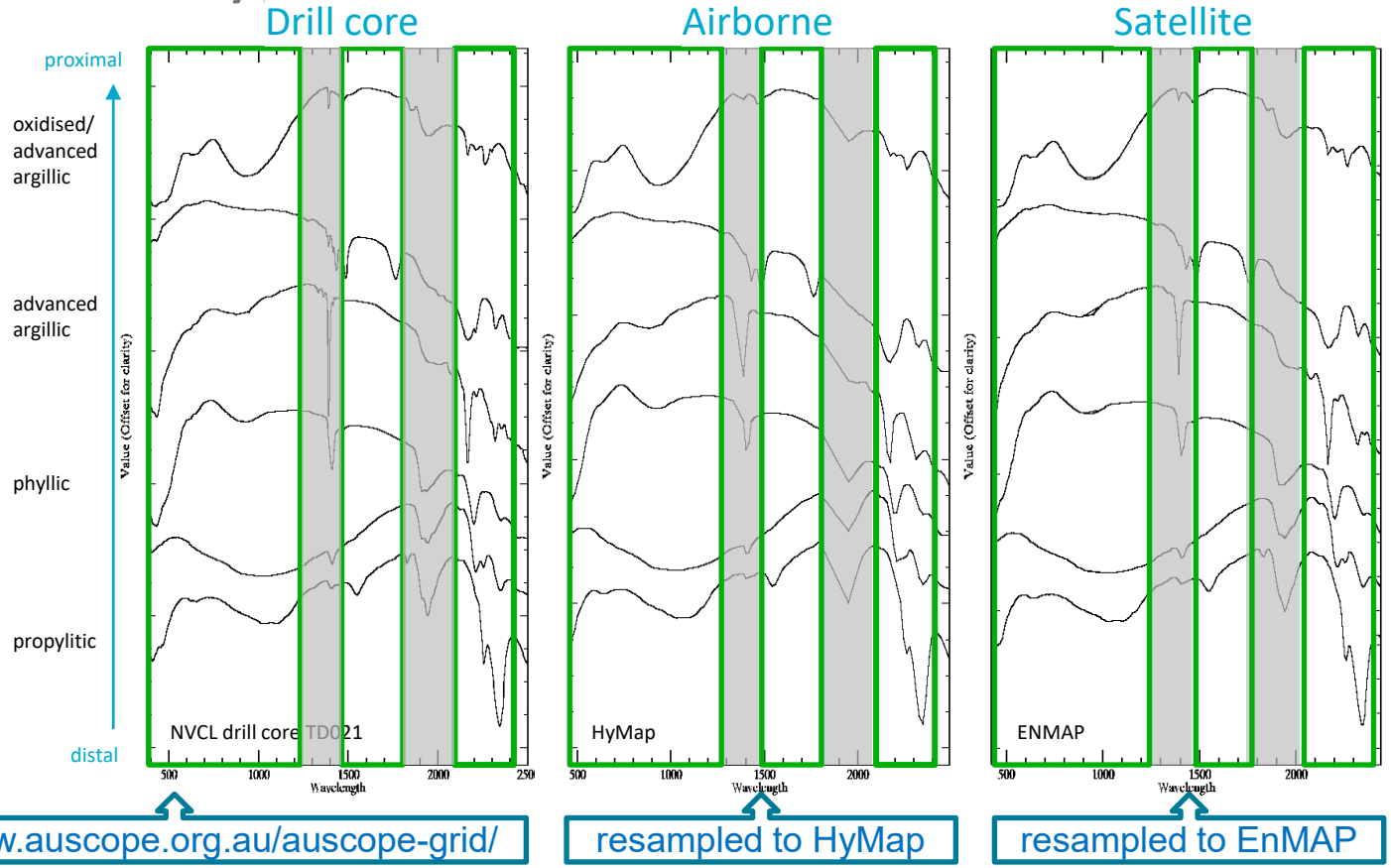

Hyper and multispectral sensors

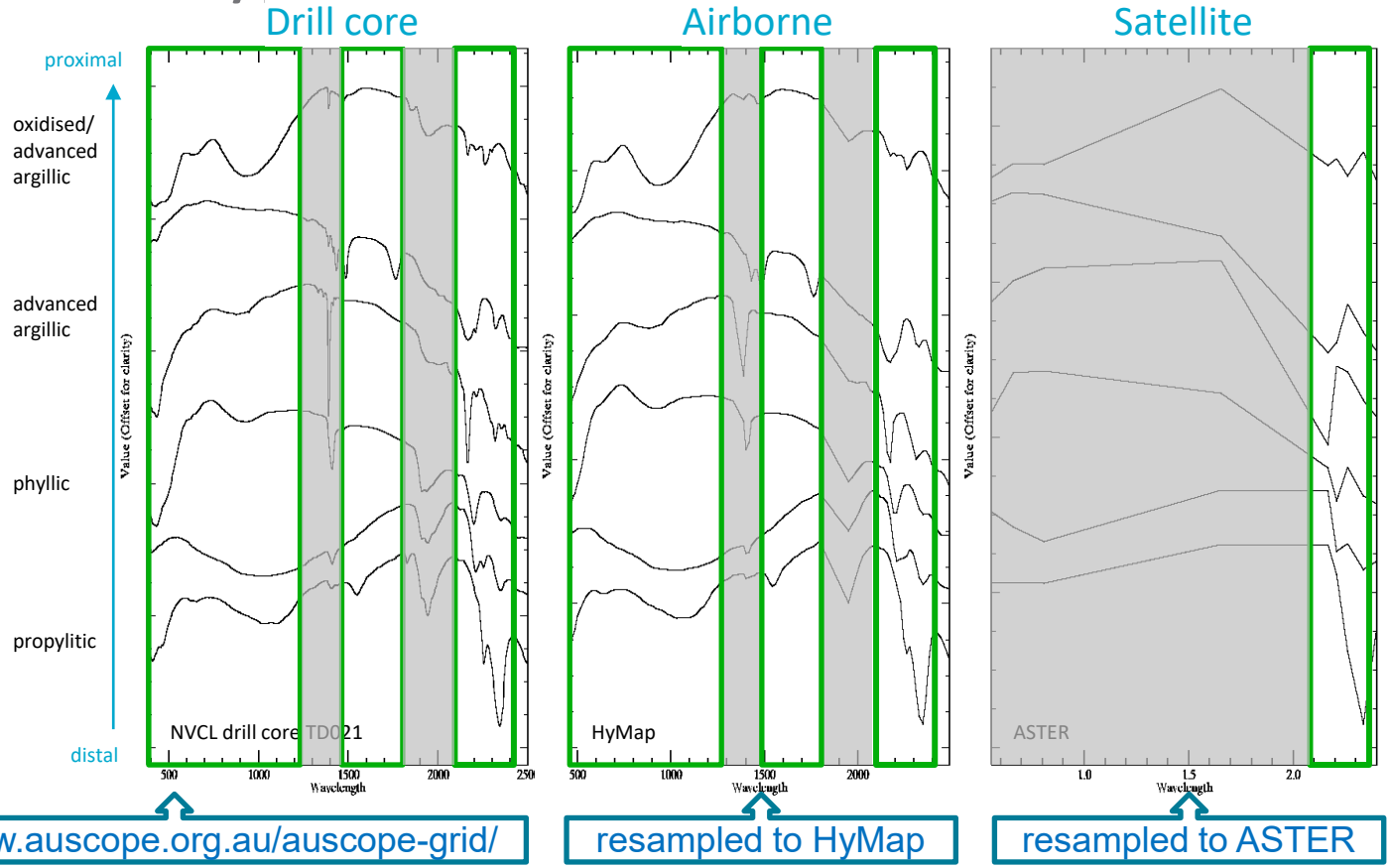

PRISMA processing workflow – Al-sheetsilicate abundance index (ASai)

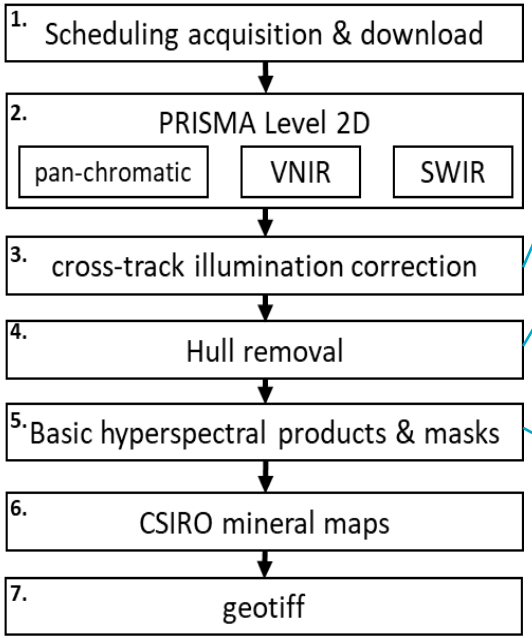

PRISMA processing workflow

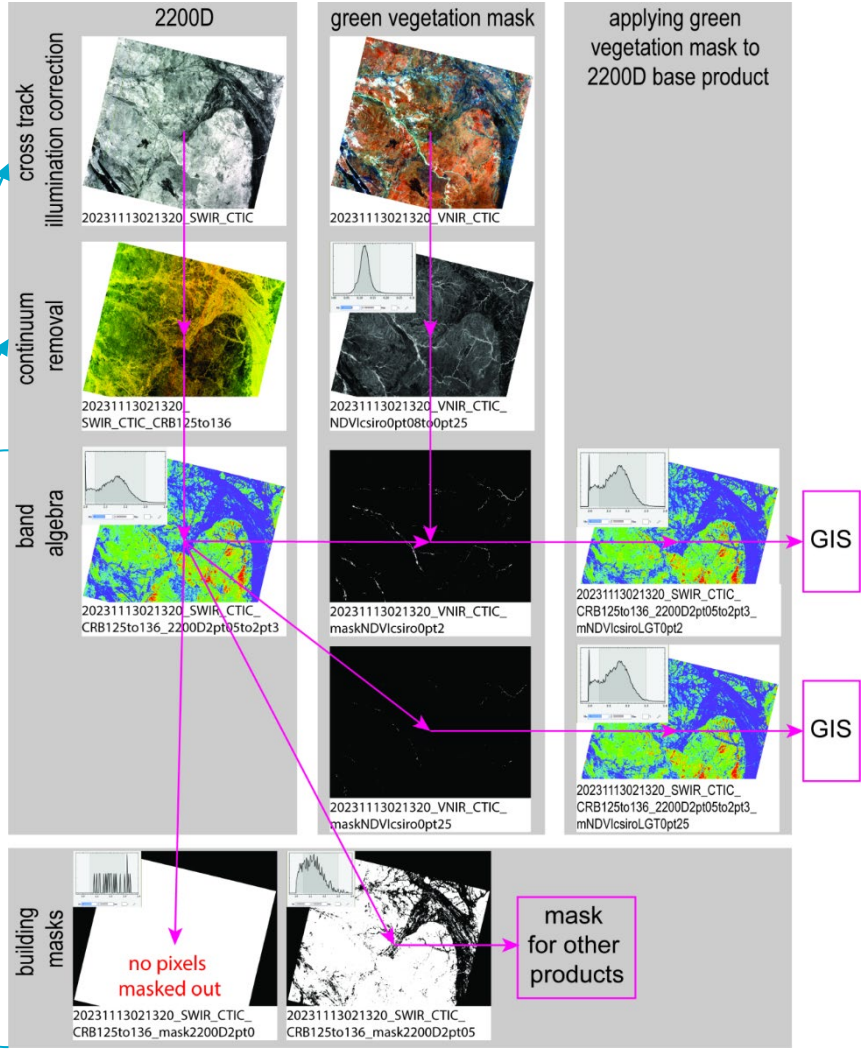

Pilbara Craton

- large, domal, multiphase granitoid-gneiss complexes (red) bordered by synformal to monoclinal greenstone belts (green)
- Greenstone belts ages ~3560 to ~2940 (granitoids emplaced similar/slightly younger)
- Spatial, geochemical and geochronological evidence links rare metals pegmatites with emplacement of younger granite suite (e.g. Split Rock Supersuite)
- 27 pegmatite groups, some combined in districts (e.g. Wodgina pegmatites)

(Sweetapple & Collins, 2002, & references therein)

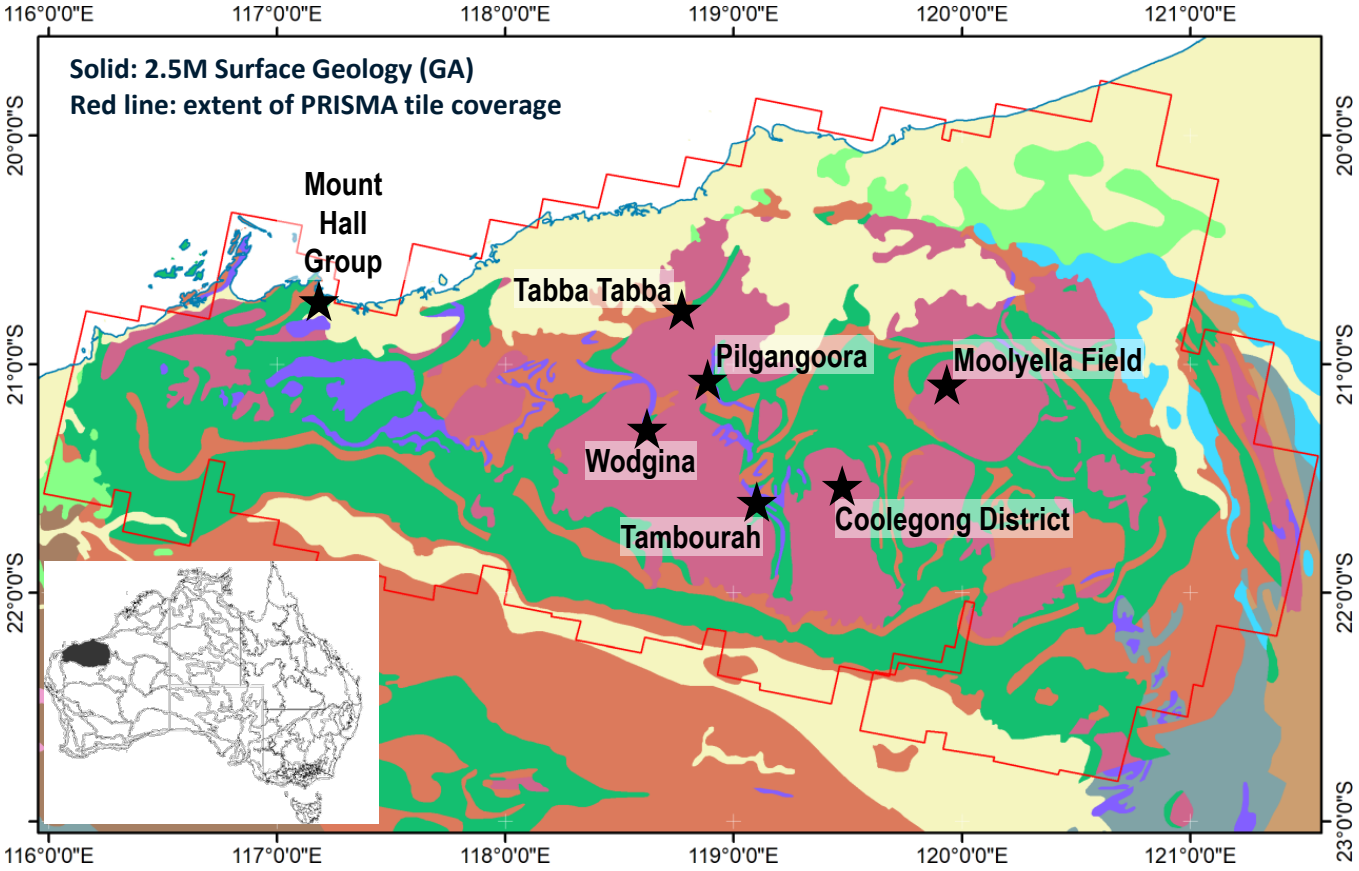

Pilbara – ASTER – Al-sheetsilicate abundance Index

- Multispectral ASTER mineral maps

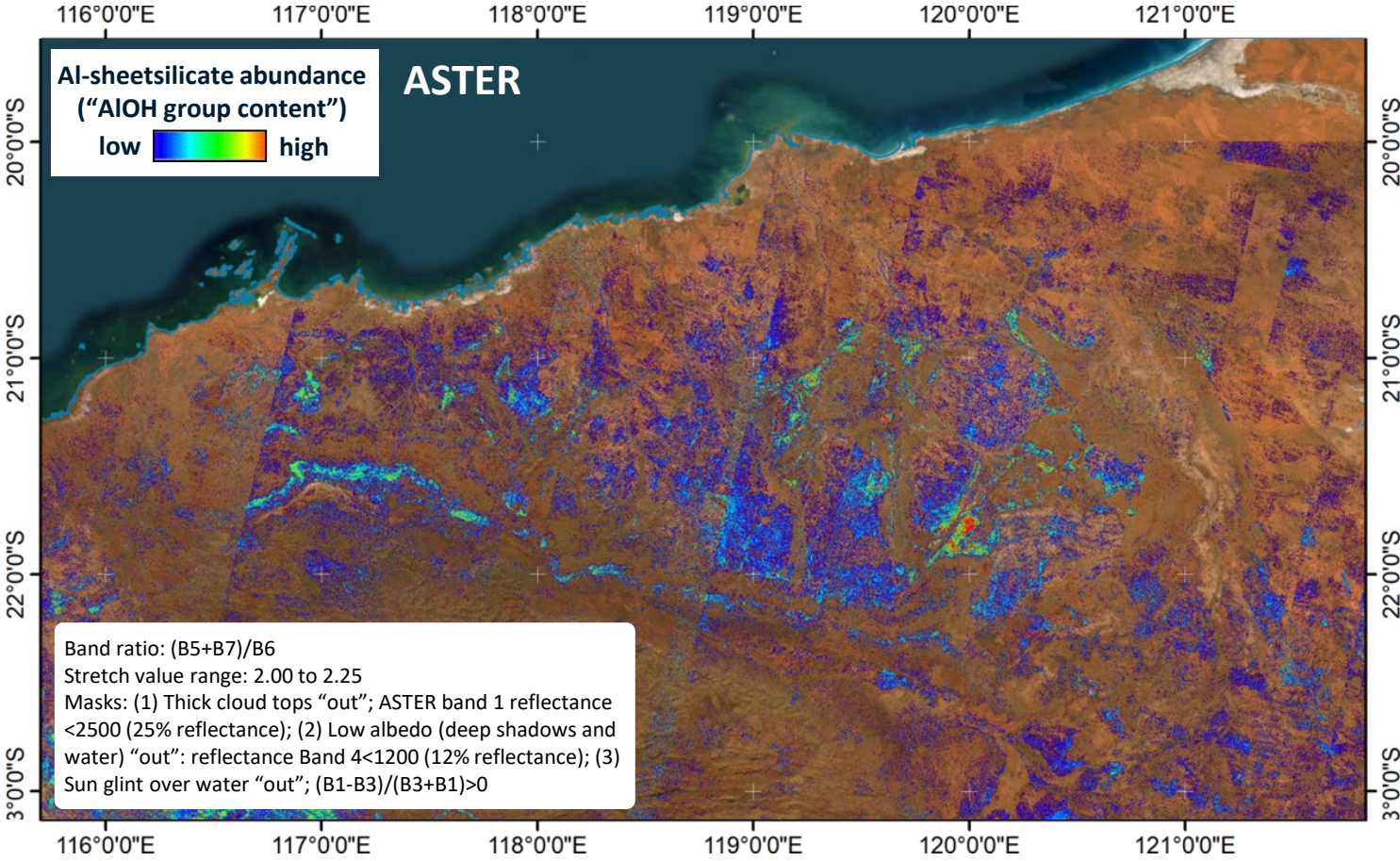

Cudahy et al. (2012), Caccetta et al. (2013)

Pilbara – PRISMA – Al-sheetsilicate abundance Index

- 250 tiles collected by means of PRISMA hyperspectral satellite sensor were processed to produce Pilbara craton-scale mineral maps
- Al-sheetsilicate abundance index shows the relative abundance of white mica, kaolinite and Al-smectite
- Different SWIR-active absorption features can be used for mapping Archean seafloor alteration (next slides)

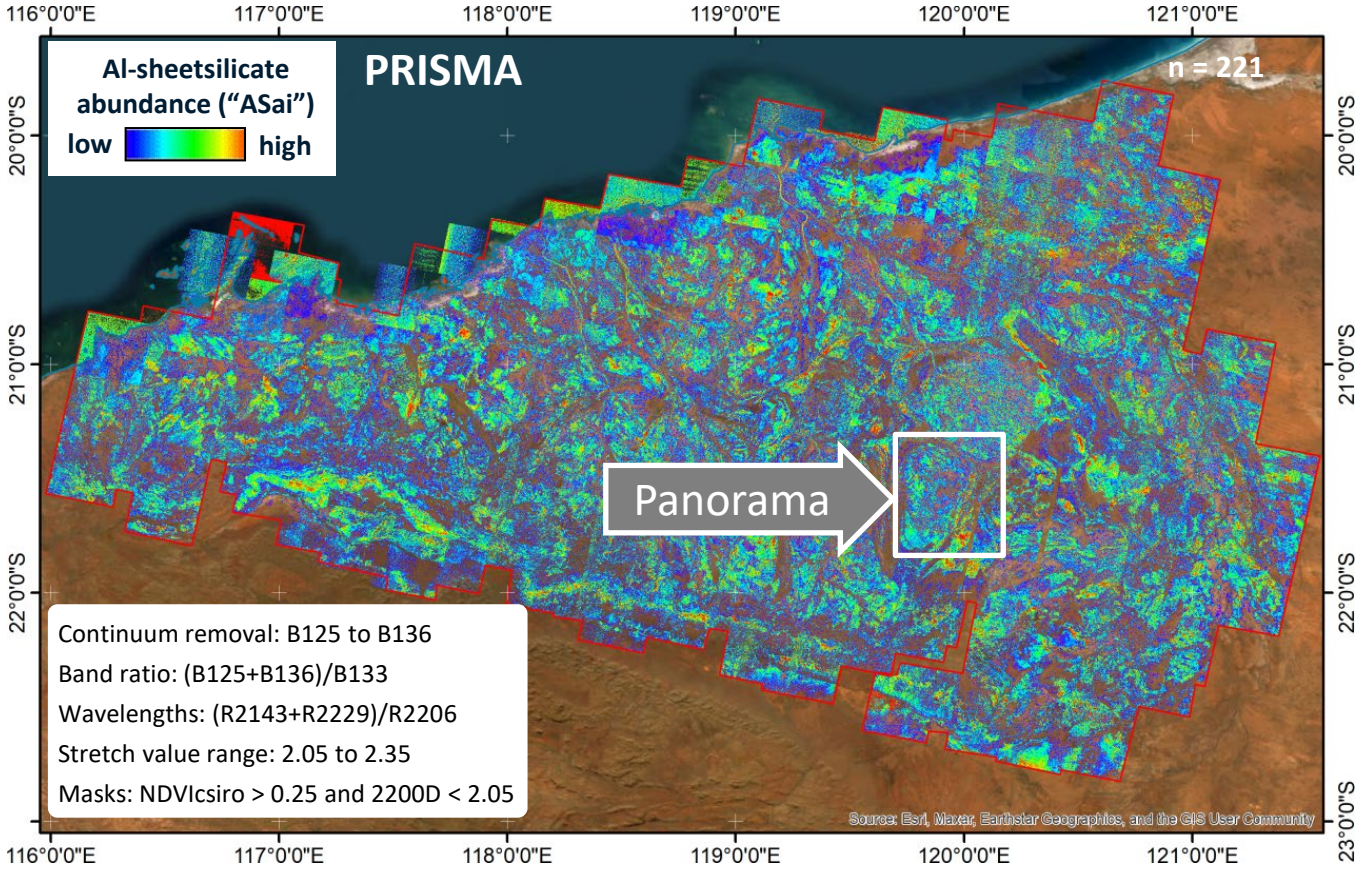

Panorama, Pilbara: White mica composition & hydrothermal alteration patterns

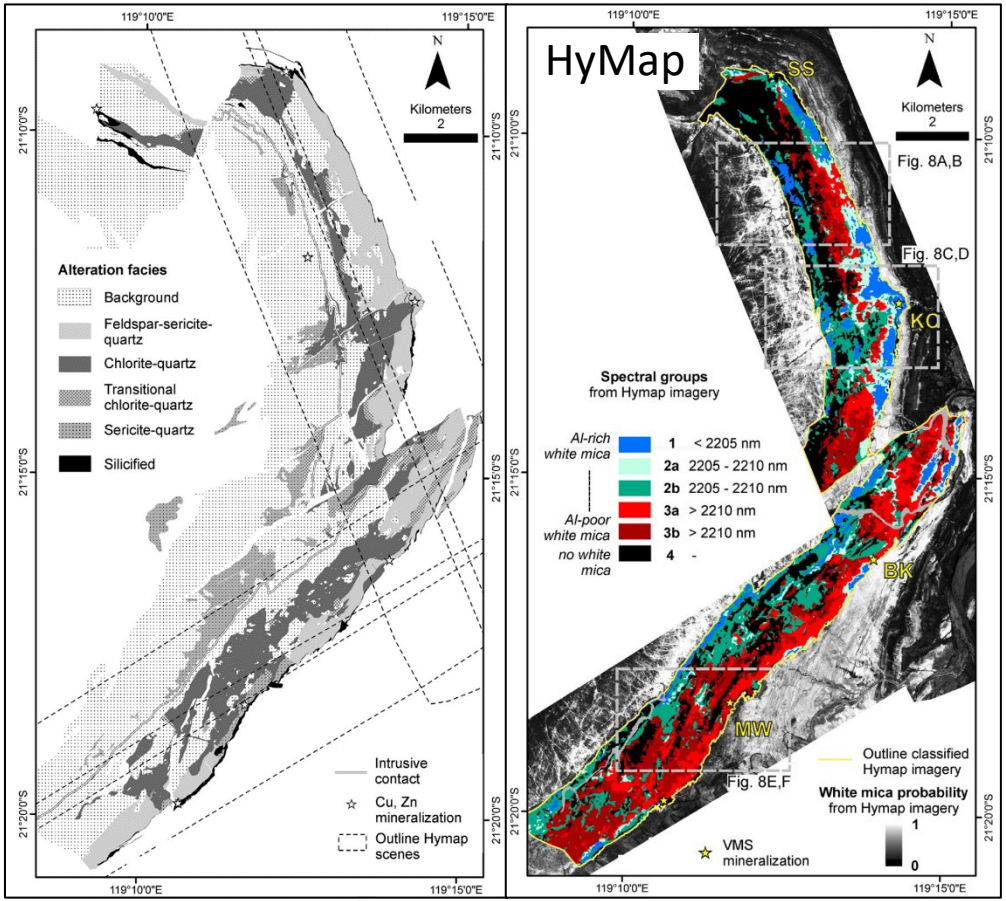

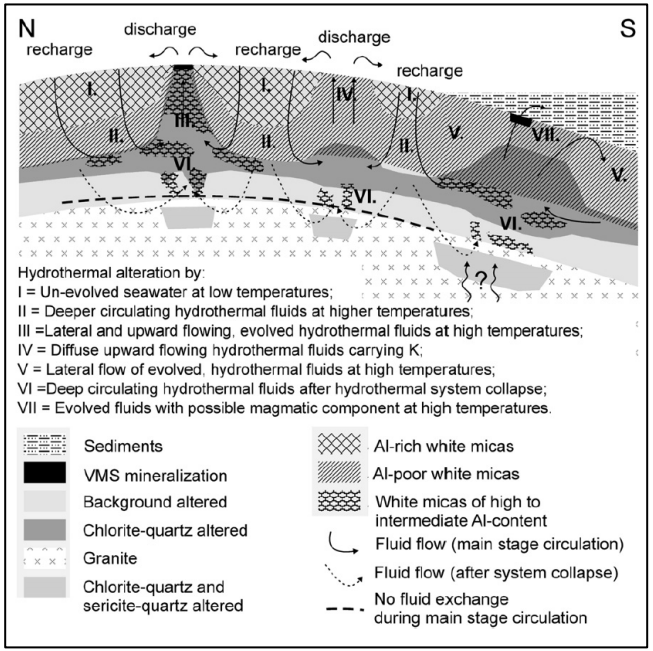

Conceptual model of (paleo) fluid flow and associated hydrothermal alteration in submarine volcanic sequence in the Panorama area (van Ruitenbeek et al., 2012)

Panorama, Pilbara: White mica composition & hydrothermal alteration patterns

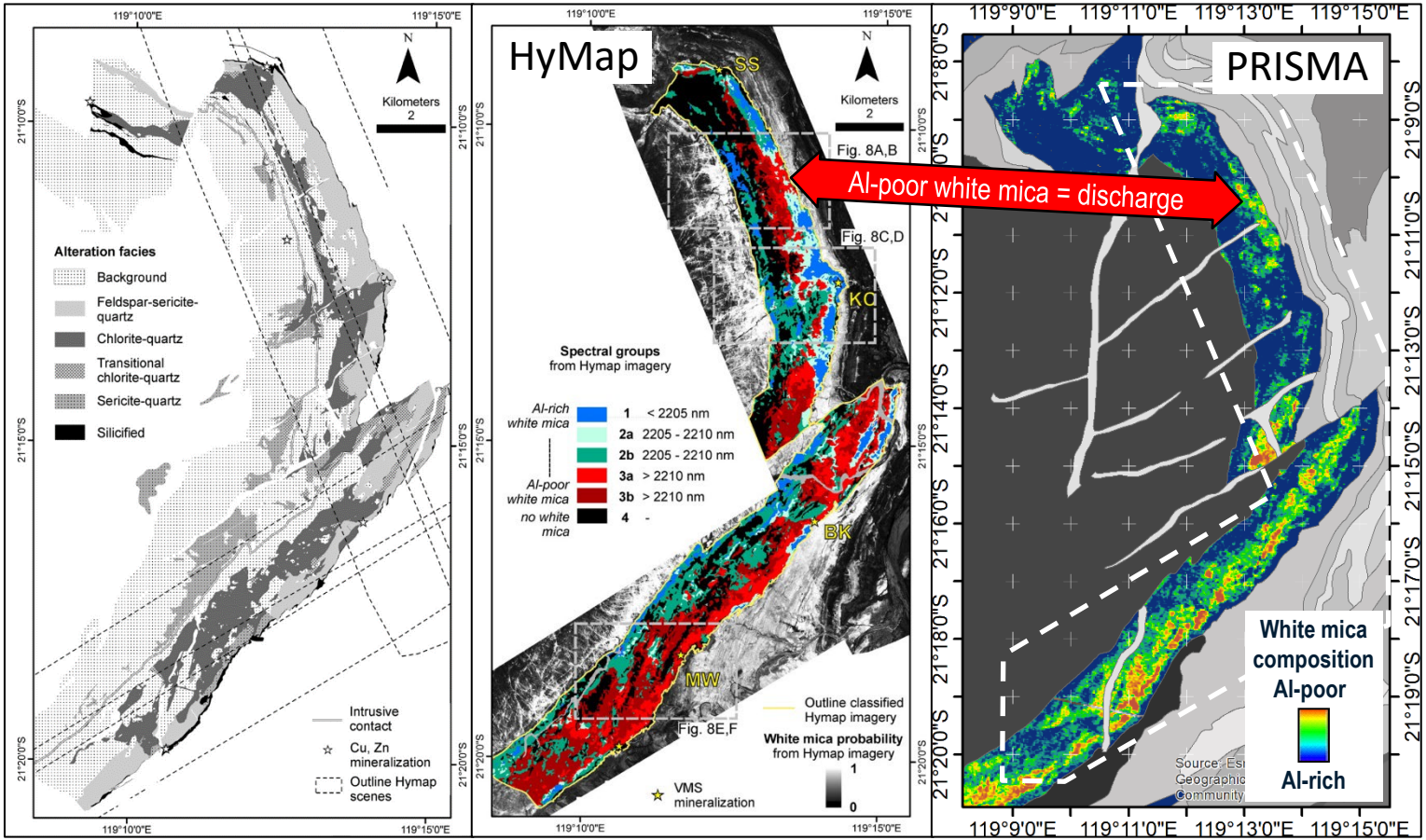

Panorama area

(Laukamp et al., in prep)

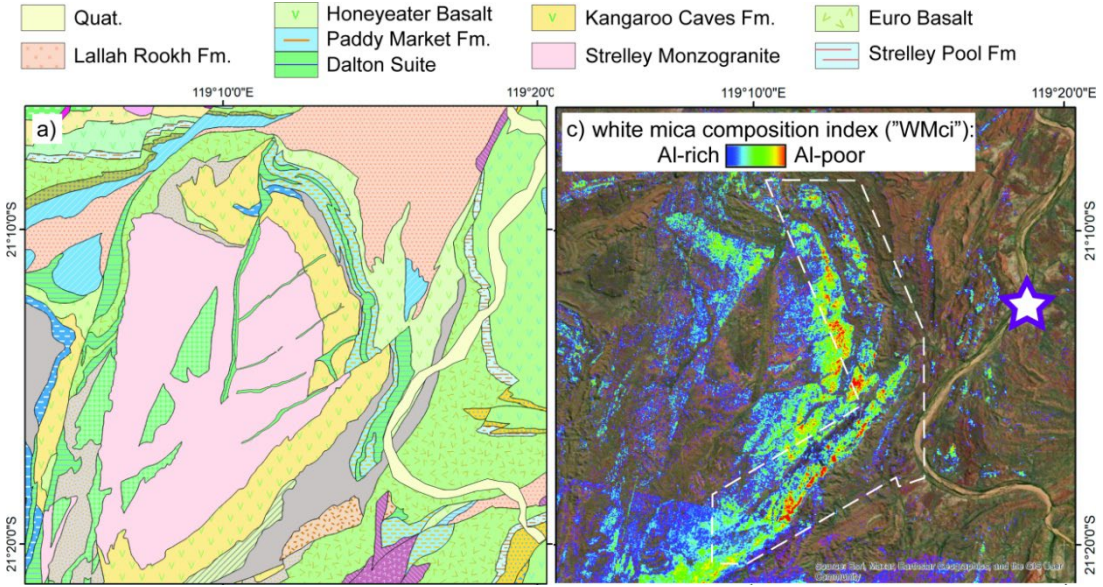

(van Ruitenbeek et al., 2012)

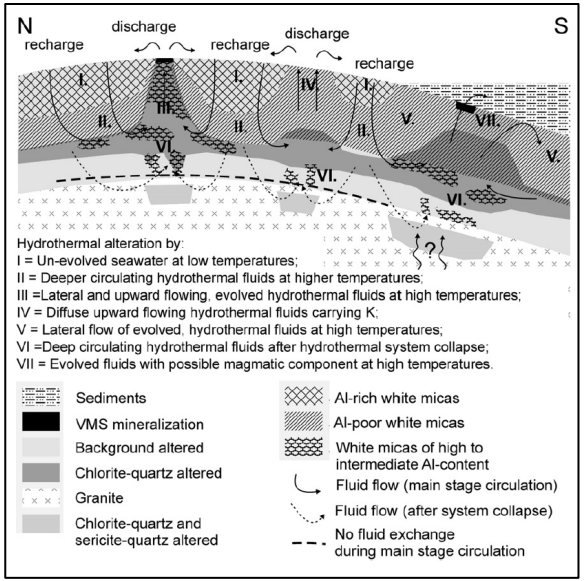

- Van Ruitenbeek et al. (2006) observed white mica compositional changes in the Kangaroo Caves Fm. in airborne hyperspectral imagery, mapping (paleo) fluid flow patterns associated with hydrothermal alteration in submarine volcanic sequences.
- Fluid recharge zones are characterised by Al-rich white mica, whereas outflow zones are identified by Al-poor white mica, due to replacement of Al by Fe and/or Mg when the fluids migrated through mafic rocks.
- The PRISMA-derived white mica composition index maps the same distribution of Al-rich and Al-poor white micas

Panorama area - Kaolinite & Pyrophyllite abundance

(Laukamp et al., in prep)

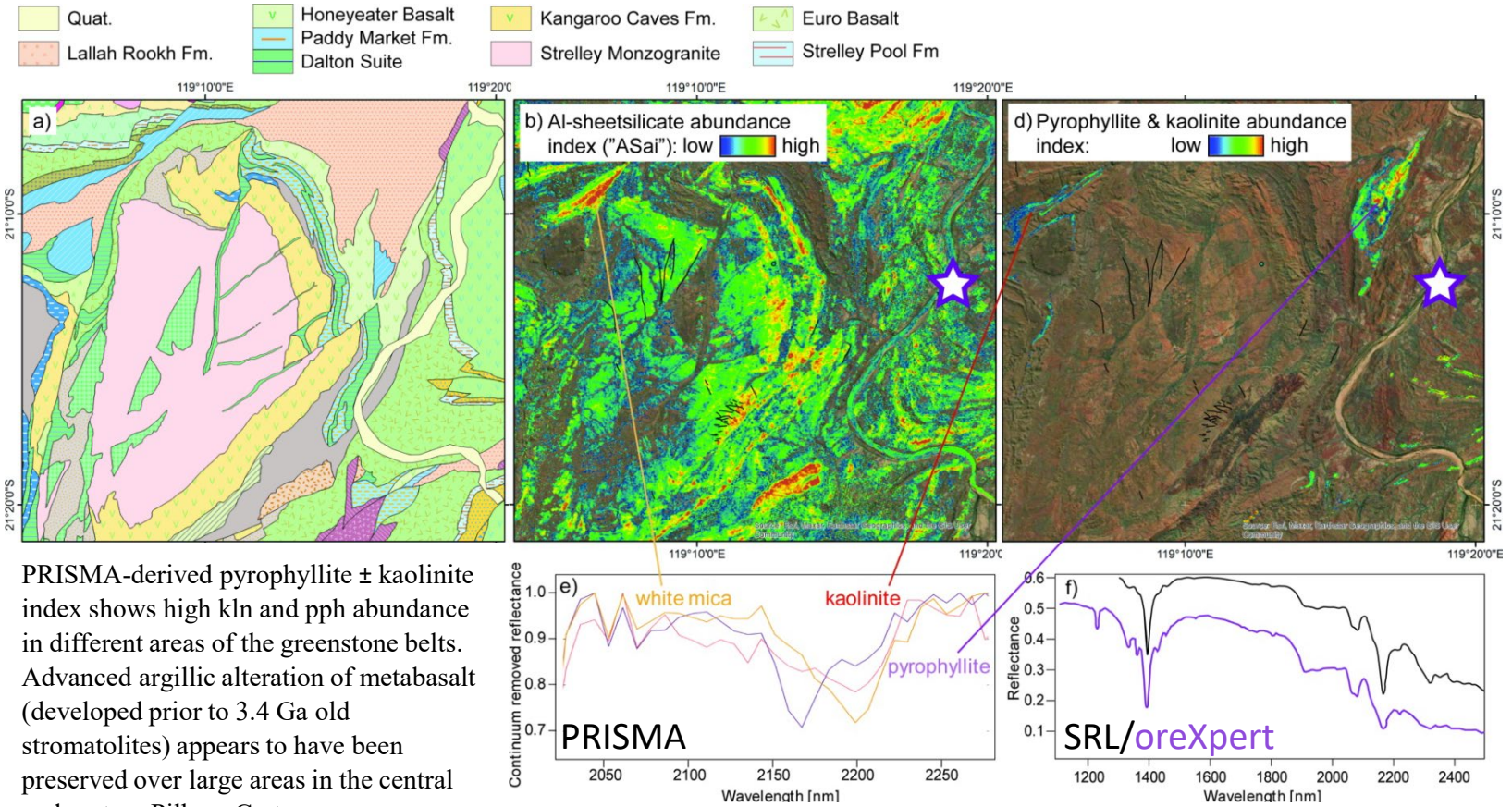

- PRISMA-derived pyrophyllite ± kaolinite index shows high kln and pph abundance in different areas of the greenstone belts.
- Advanced argillic alteration of metabasalt (developed prior to 3.4 Ga old stromatolites) appears to have been preserved over large areas in the central and eastern Pilbara Craton.

Rocklea Dome – Airborne hyperspectral

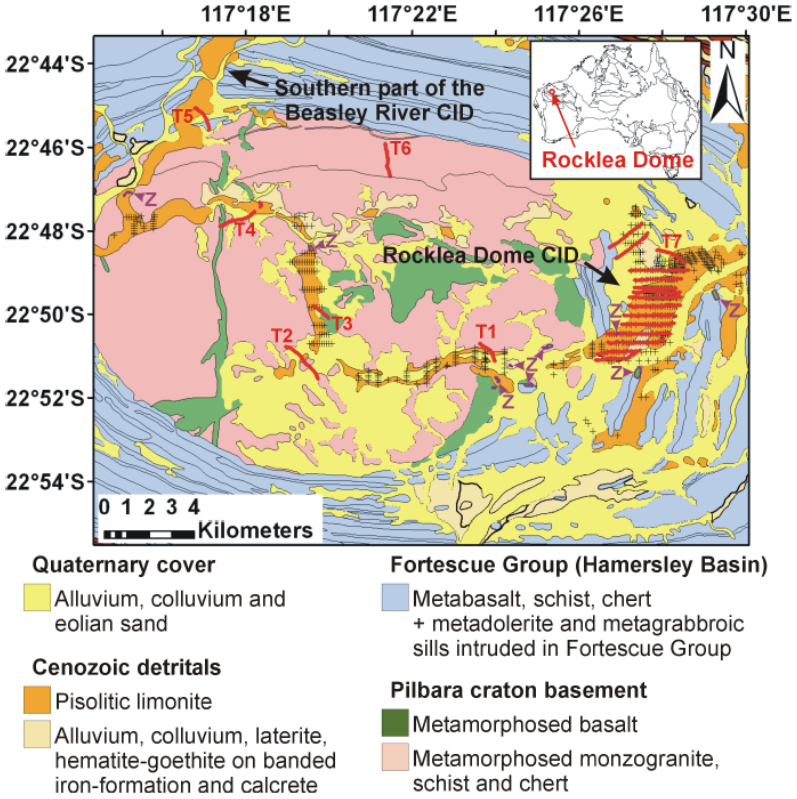

Modified after Haest et al. (2012)

White mica abundance index

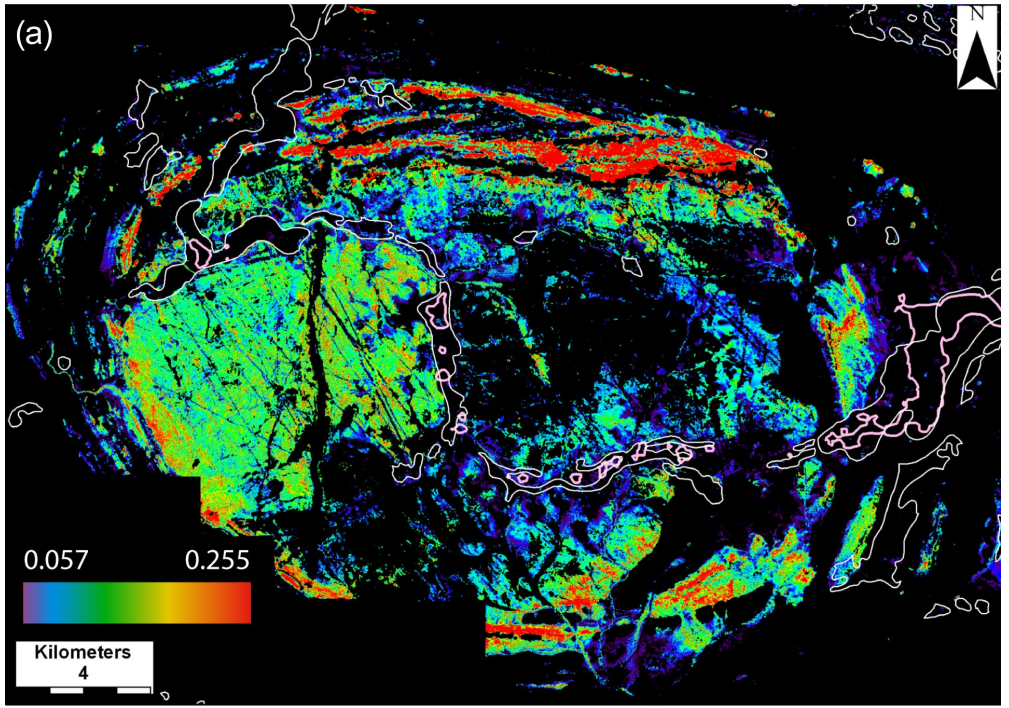

Laukamp et al. (2021)

Rocklea Dome – Airborne hyperspectral

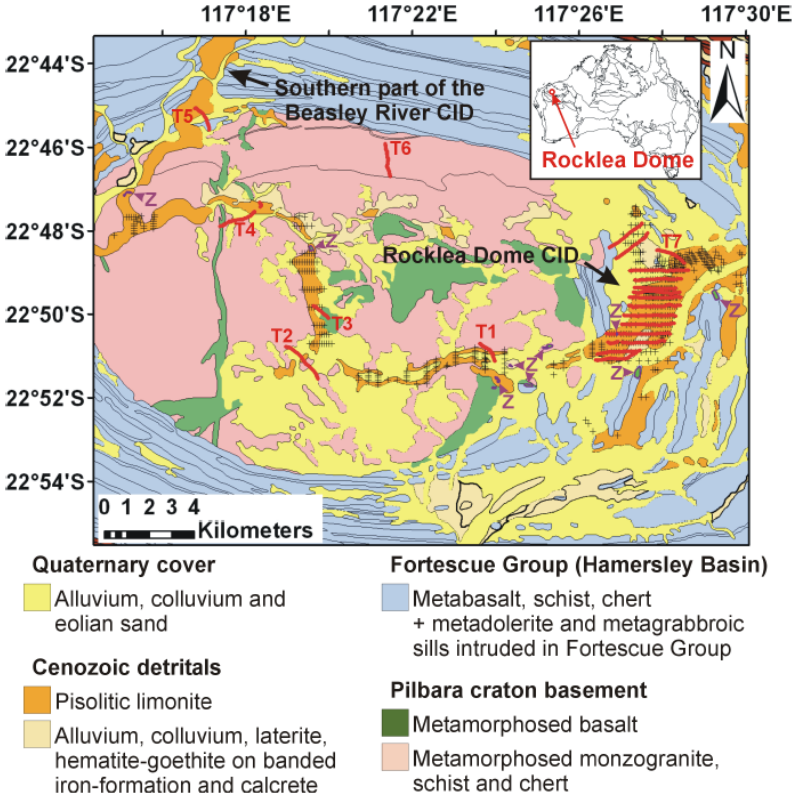

Modified after Haest et al. (2012)

Chlorite abundance index

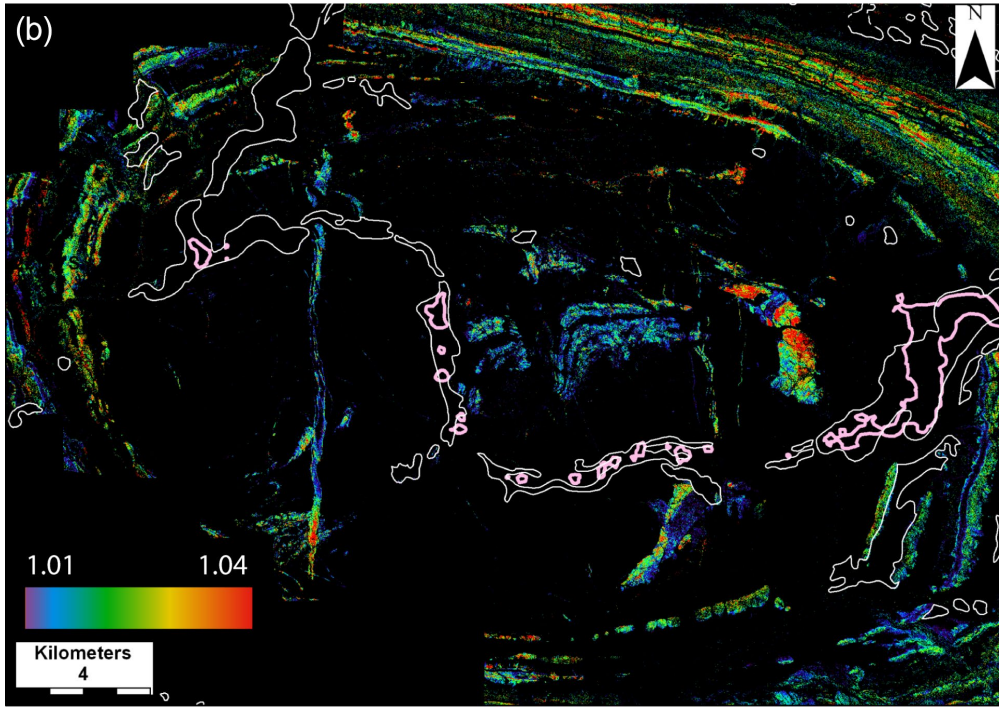

Laukamp et al. (2021)

Kaolin crystallinity

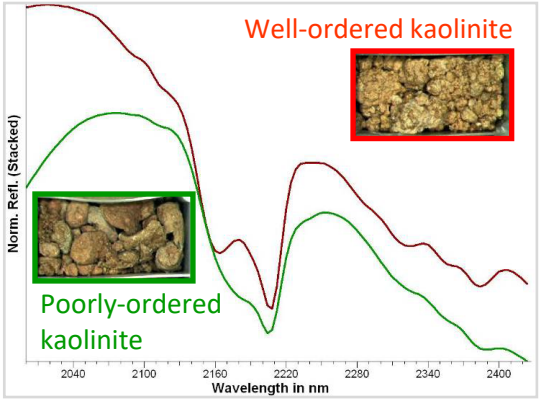

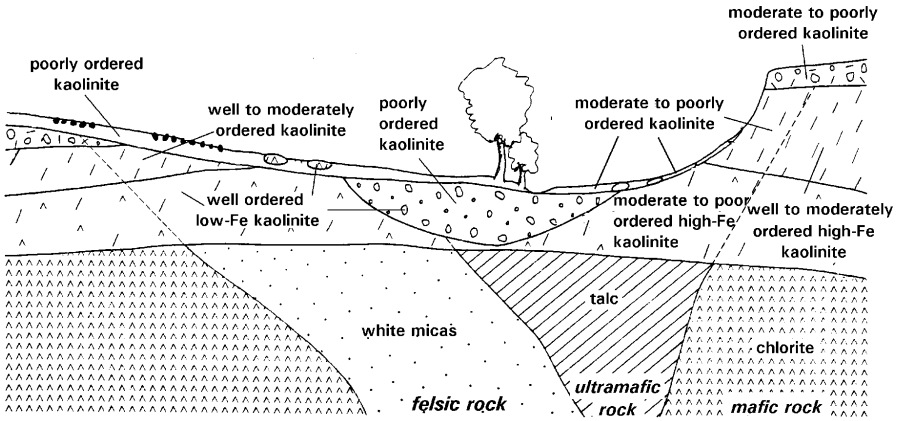

(from Cudahy et al., 2005, and others)

Cudahy et al. (2005)

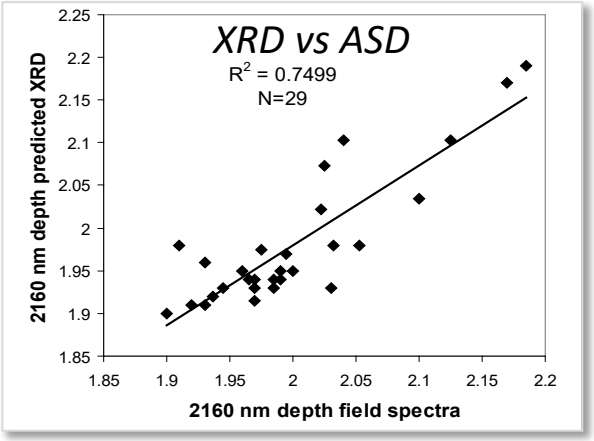

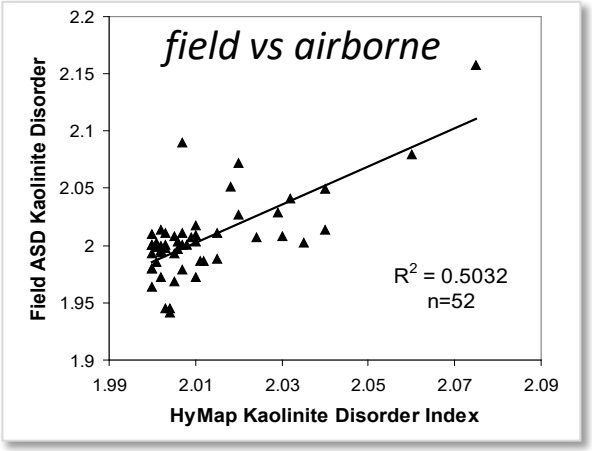

Rocklea Dome – Drill core, airborne & satellite hyperspectral

Hyperspectral 3D Mineral Map

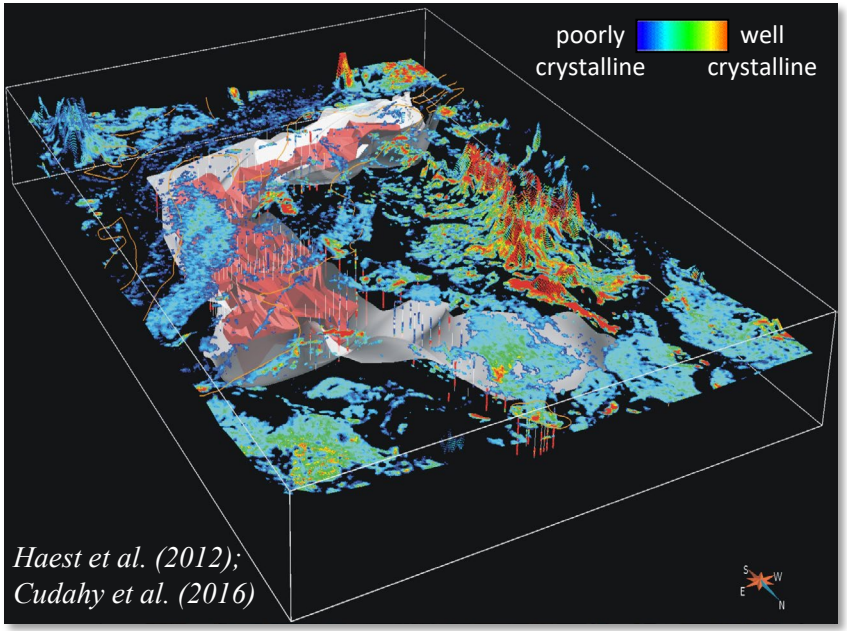

Surface: Airborne hyperspectral-derived kaolin crystallinity (rainbow colour stretch)
White polygon: Tertiary channel boundary based on drill core hyperspectral-derived kaolin crystallinity. Red polygon: Channel Iron Ore resource
Vertical strings are drill holes, coloured by hyperspectral-derived kaolin crystallinity

Kaolin crystallinity index

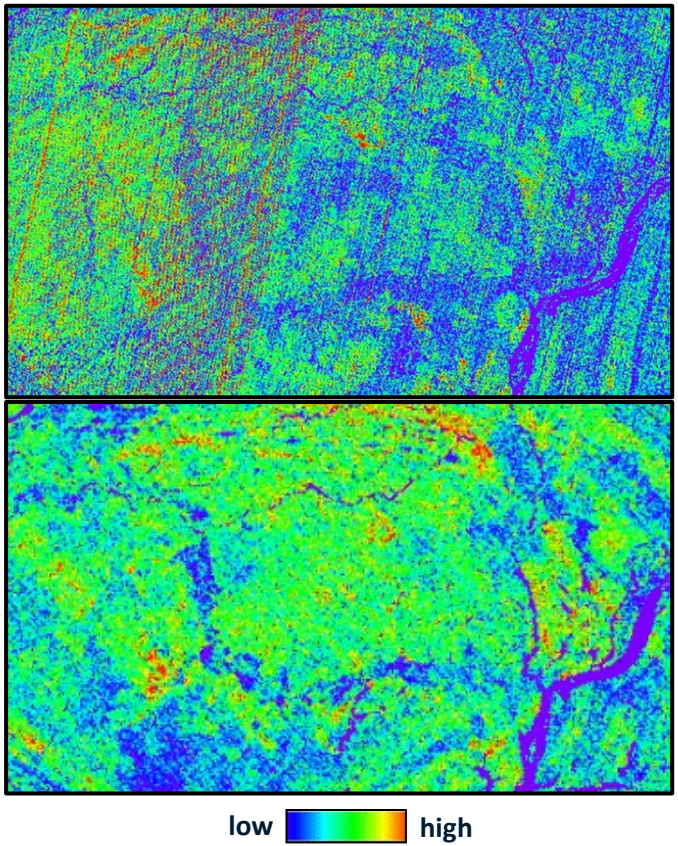

PRISMA
30 m pixel
Low SNR

EMIT
60 m pixel
High SNR

Rocklea Dome – Satellite hyperspectral

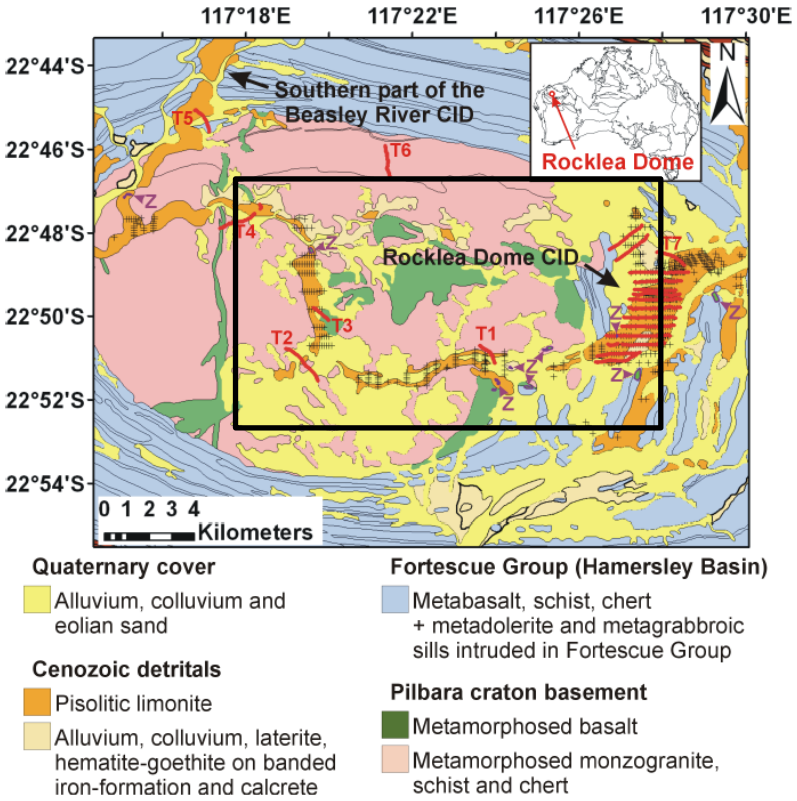

Modified after Haest et al. (2012)

Kaolin crystallinity index

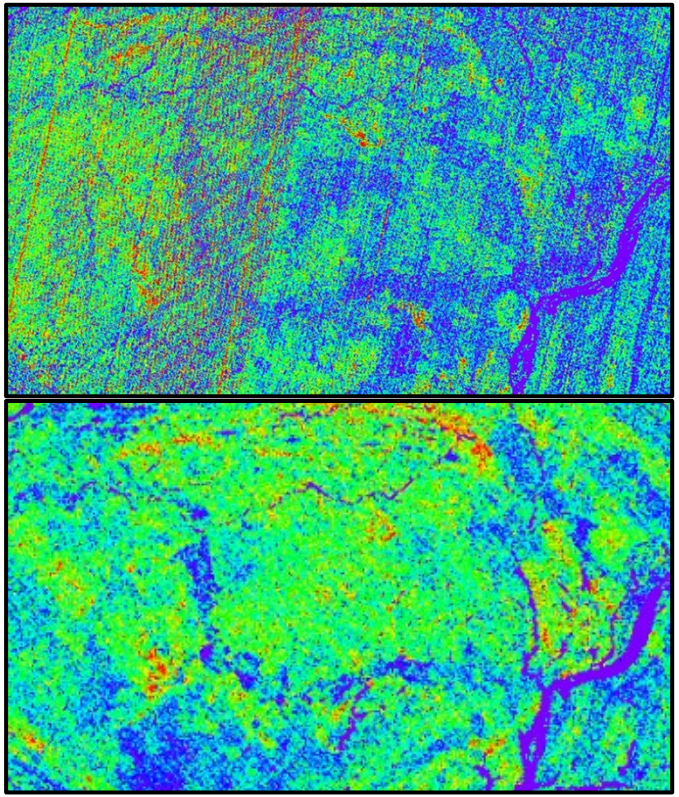

PRISMA
30 m pixel
Low SNR

EMIT
60 m pixel
High SNR

Rocklea Dome – Satellite hyperspectral

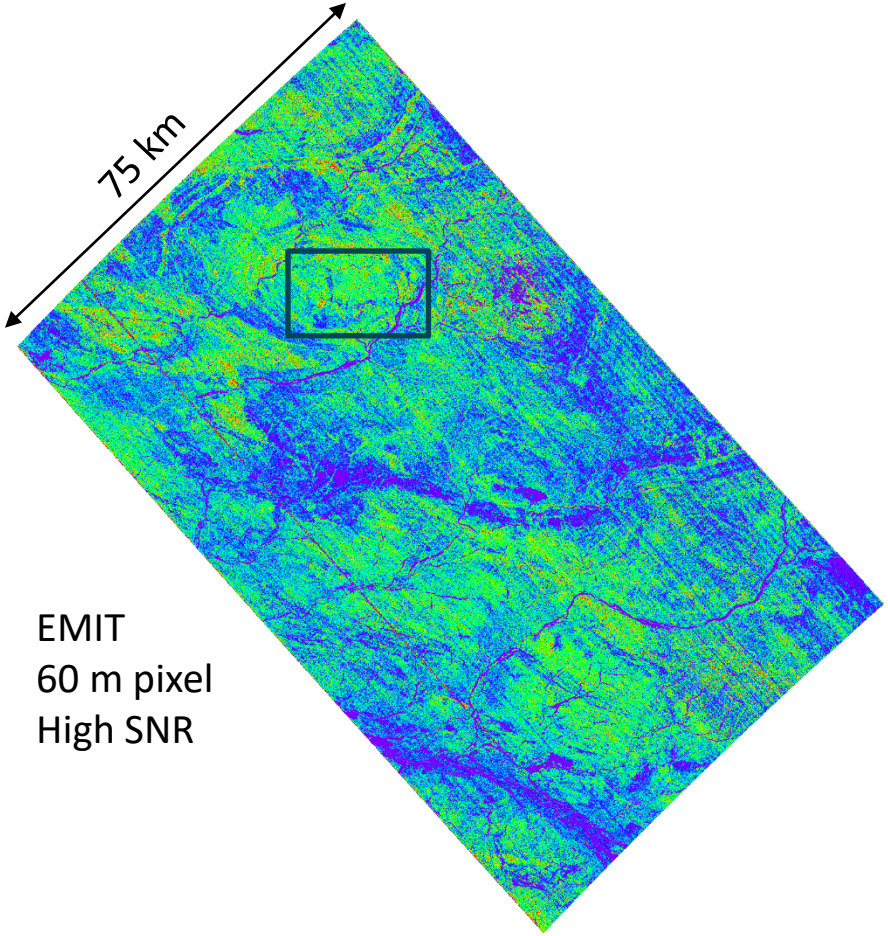

EMIT
60 m pixel
High SNR

Kaolin crystallinity index

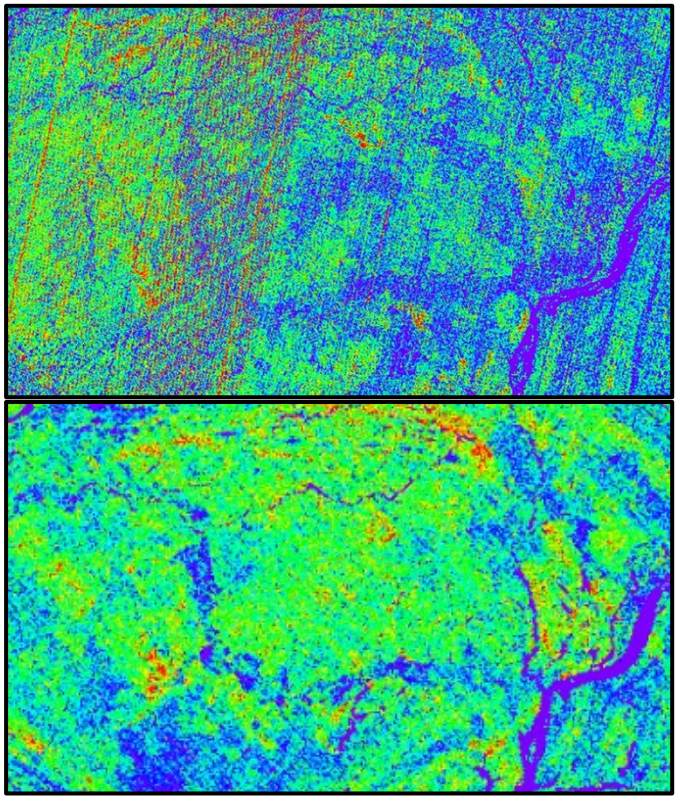

PRISMA
30 m pixel
Low SNR

EMIT
60 m pixel
High SNR

Summary

- Comparison of mineral maps derived from satellite hyperspectral imagery with those processed from multispectral satellite imagery (i.e. ASTER) shows that the higher spectral resolution of the new sensors increases the level of confidence when assigning pixels to the respective mineral groups.
- Therefore, masking thresholds in the band ratio decision tree can be relaxed, improving the coverage of classified pixels, important for: 1) recognition of regional mineral patterns that are only retrievable from the SWIR, and 2) identification of important critical metal host rocks, such as pegmatites, down to the tenement-scale.
- Satellite hyperspectral imagery enables craton- to tenement-scale mapping of the relative abundance of Al-sheetsilicates and even Fe,Mg-sheetsilicates, as well as their compositional variations.
- Satellite imagery-based mapping of kaolin crystallinity challenging, but sufficient for regolith landform classification.
- Publicly available hyperspectral imagery covering the TIR (and MIR!?) wavelength range required!

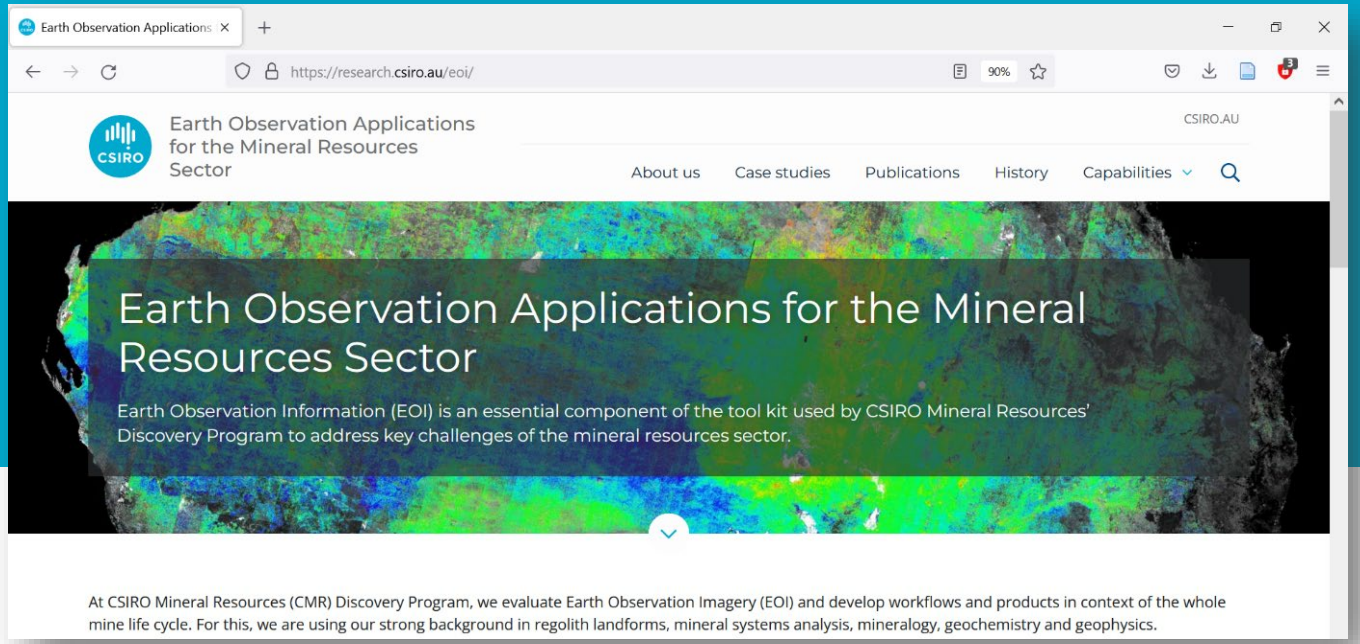

Thank you

CSIRO Mineral Resources
Carsten Laukamp
Principal Research Scientist

carsten.laukamp@csiro.au

Government of Western Australia
Department of Mines and Petroleum

AUSTRALASIAN METALS

KoBold Metals

CSIRO

Regional-scale mapping of phyllosilicates using the new generation of VNIR-SWIR hyperspectral satellite sensors

Laukamp, Carsten*1, Lau, Ian C.1, Lampinen, Heta M.1, Williams, M.1, and Huang, Fang1

The latest generation of optical satellite sensors that collect reflectance spectra from across the visible-near infrared (VNIR, 380 to 1000 nm) and shortwave infrared (SWIR, 1000 to 2500 nm) wavelength region at hyperspectral resolution enable the regional-scale mapping of phyllosilicates at unprecedented detail. Typically, these new satellite hyperspectral sensors have a spectral sampling interval of about 10 nm in the SWIR, at a pixel size of 30 m, such as in the case of PRISMA (www.asi.it/en/earth-science/prisma/) and EnMap (https://www.enmap.org/), or 60 m for EMIT (https://earth.jpl.nasa.gov/emit/). The high spectral resolution across the SWIR allows the identification of combinations of the bending and stretching fundamentals of hydroxyl groups, which produce diagnostic spectral signatures of Al-phyllosilicates (e.g. kaolin, white mica, Al-smectite, pyrophyllite) as well as Fe-Mg-phyllosilicates (e.g. chlorite).

This paper provides examples of mapping the relative abundance, compositional variation and crystallinity of Al-phyllosilicates across geological provinces from the regional to kilometer-scale, describing its geological significance and application for critical metals exploration. For example, simple three-band ratios that target the relative depths and wavelength positions of major absorptions centered at around 2160 and 2200 nm are combined to infer the relative abundance and crystallinity of kaolinite, which supports the classification of in-situ versus transported regolith. The regolith classification helps with the identification of shallow regolith and potential sub-cropping areas, but also improves delineation of catchment areas. In greenstone belts of the central and eastern Pilbara craton (Western Australia), an elevated pyrophyllite abundance is highlighted by pixels with the strongest 2160 nm absorptions, providing insights into the extent of Archean hydrothermal alteration patterns that are potentially associated with mineral deposits.

The comparison of mineral maps derived from the satellite hyperspectral imagery with earlier developed mineral maps processed from multispectral satellite imagery (i.e. ASTER) shows that the higher spectral resolution of the new sensors also increases the level of confidence when assigning pixels to the respective mineral groups. Therefore, masking thresholds in the band ratio decision tree can be relaxed, improving the coverage of classified pixels. This is important for both the recognition of regional mineral patterns that are only retrievable from the SWIR, but also the identification of important critical metal host rocks, such as pegmatites, down to the tenement-scale.

References

- Cudahy, T., Caccetta, M., Thomas, M., Hewson, R., Abrams, M., Kato, M., Kashimura, O., Ninomiya, Y., Yamaguchi, Y., Collings, S., Laukamp, C., Ong, C., Lau, I., Rodger, A., Chia, J., Warren, P., Woodcock, R., Fraser, R., Rankine, T., Vote, J., de Caritat, P., English, P., Meyer, D., Doescher, C., Fu, B., Shi, P., Mitchell, R., 2016. Satellite-derived mineral mapping and monitoring of weathering, deposition and erosion. Sci Rep 6, 23702. https://doi.org/10.1038/srep23702
- Cudahy, T.J., Caccetta, M., Cornelius, A., Hewson, R., Wells, M., Skwarnecki, M., Halley, S., Hausknecht, P., Mason, P., Quigley, M., 2005. Regolith, geology and alteration mineral maps from new generation airborne and satellite remote sensing technologies: results of research carried out as MERIWA Project no. M370. MERIWA, East Perth, WA.
- Haest, M., Cudahy, T., Laukamp, C., Gregory, S., 2012a. Quantitative Mineralogy from Infrared Spectroscopic Data. I. Validation of Mineral Abundance and Composition Scripts at the Rocklea Channel Iron Deposit in Western Australia. Economic Geology 107, 209–228. https://doi.org/10.2113/econgeo.107.2.209
- Haest, M., Cudahy, T., Laukamp, C., Gregory, S., 2012b. Quantitative Mineralogy from Infrared Spectroscopic Data. II. Three-Dimensional Mineralogical Characterization of the Rocklea Channel Iron Deposit, Western Australia. Economic Geology 107, 229–249. https://doi.org/10.2113/econgeo.107.2.229
- Laukamp, C., Haest, M., Cudahy, T., 2021. The Rocklea Dome 3D Mineral Mapping Test Data Set. Earth Syst. Sci. Data 13, 1371–1383. https://doi.org/10.5194/essd-13-1371-2021
- Sweetapple, M.T., Collins, P.L.F., 2002. Genetic Framework for the Classification and Distribution of Archean Rare Metal Pegmatites in the North Pilbara Craton, Western Australia. Economic Geology 97, 873–895. https://doi.org/10.2113/gsecongeo.97.4.873
- Van Ruitenbeek, F.J.A., Cudahy, T.J., Van Der Meer, F.D., Hale, M., 2012. Characterization of the hydrothermal systems associated with Archean VMS-mineralization at Panorama, Western Australia, using hyperspectral, geochemical and geothermometric data. Ore Geology Reviews 45, 33–46. https://doi.org/10.1016/j.oregeorev.2011.07.001